



Published in final edited form as:

Autism Res. 2010 December ; 3(6): 350–358. doi:10.1002/aur.162.

Atypical Diffusion Tensor Hemispheric Asymmetry in Autism

Nicholas Lange^{1,2,3}, Molly B. DuBray^{4,5}, Jee Eun Lee⁶, Michael P. Froimowitz^{1,3}, Alyson Froehlich⁴, Nagesh Adluru⁶, Brad Wright⁷, Caitlin Ravichandran^{1,8}, P. Thomas Fletcher^{9,10,11}, Erin D. Bigler^{4,11,12,13}, Andrew L. Alexander^{6,14,15}, and Janet E. Lainhart^{4,5,7,11}

¹Department of Psychiatry, Harvard Medical School, Boston, MA, USA

²Department of Biostatistics, Harvard School of Public Health, Boston, MA, USA

³Neurostatistics Laboratory, McLean Hospital, Belmont, MA, USA

⁴Department of Psychiatry, School of Medicine, University of Utah, Salt Lake City, UT, USA

⁵Interdepartmental Neuroscience Program, University of Utah, Salt Lake City, UT, USA

⁶Waisman Laboratory for Brain Imaging and Behavior, University of Wisconsin, Madison, WI, USA

⁷School of Medicine, University of Utah, Salt Lake City, UT, USA

⁸Laboratory for Psychiatric Biostatistics, McLean Hospital, Belmont, MA, USA

⁹School of Computing, University of Utah, Salt Lake City, UT

¹⁰Scientific Computing and Imaging Institute, University of Utah, Salt Lake City, UT

¹¹The Brain Institute at the University of Utah, Salt Lake City, UT

¹²Department of Psychology, Brigham Young University, Provo, UT, USA

¹³Neuroscience Center, Brigham Young University, Provo, UT, USA

¹⁴Department of Medical Physics, University of Wisconsin, Madison, WI, USA

¹⁵Department of Psychiatry, University of Wisconsin, Madison, WI, USA

Abstract

Background—Biological measurements that distinguish individuals with autism from typically developing individuals and those with other developmental and neuropsychiatric disorders must demonstrate very high performance to have clinical value as potential imaging biomarkers. We hypothesized that further study of white matter microstructure (WMM) in the superior temporal gyrus (STG) and temporal stem (TS), two brain regions in the temporal lobe containing circuitry central to language, emotion and social cognition, would identify a useful combination of classification features and further understand autism neuropathology.

Methods—WMM measurements from the STG and TS were examined from thirty high-functioning males satisfying full criteria for idiopathic autism aged 8–26 years and 30 matched controls and a replication sample of 12 males with idiopathic autism and 7 matched controls that

Corresponding Author: Nicholas Lange, McLean Hospital, 115 Mill Street, Belmont, MA 02478 USA, nlange@hms.harvard.edu, Telephone: (617) 855-2139, Fax: (617) 855-4040.

FINANCIAL DISCLOSURES

The authors report no biomedical financial interests or potential conflicts of interest.

participated in a previous case-control diffusion tensor imaging (DTI) study. Language functioning, adaptive functioning and psychotropic medication usage were also examined.

Results—In the STG, we find reversed hemispheric asymmetry of two separable measures of directional diffusion coherence. Tensor skewness is greater on the right in autism and fractional anisotropy is decreased on the left. We also find increased diffusion parallel to white matter fibers bilaterally. In the right not left TS we find increased omnidirectional, parallel and perpendicular diffusion. These six multivariate measurements possess very high ability to discriminate individuals with autism from individuals without autism with 94% sensitivity, 90% specificity and 92% accuracy in our original and replication samples. We also report a near-significant association between the classifier and a quantitative trait index of autism and significant correlations between two classifier components and measures of language, IQ and adaptive functioning in autism.

Keywords

Adaptive functioning; Classification; Diffusion tensor imaging; Hemispheric asymmetry; Language functioning

INTRODUCTION

Objective *in vivo* biological measurements that distinguish individuals with autism from typically developing individuals and those with other developmental neuropsychiatric disorders must demonstrate very high classification ability to have applied clinical value and elucidate neuropathology specific to autism. Biological measurements proposed to date are not yet clinically adequate and none has been replicated in an independent sample (Lainhart & Lange, in press); Table 1. The pathogenesis of autism appears to involve white matter microstructure (WMM) and atypical inter-hemispheric functioning even in the absence of volumetric differences (Bigler et al., 2007; Alexander et al, 2007; Flagg, Cardy, Roberts, & Roberts, 2005; Kleinhans, Muller, Cohen, & Courchesne, 2008; Wilson, Rojas, Reite, Teale, & Rogers, 2007; Fletcher, et al., 2010).

Diffusion tensor imaging (DTI) measures WMM by mapping directions of water diffusion in a local brain tissue frame of reference (Basser, Mattiello, & LeBihan, 1994). Each tensor is a geometrically organized set of six 3D diffusion rates summarized typically by four coefficients: fractional anisotropy (FA, directional diffusion coherence along axons, Basser & Pierpaoli, 1996; Pierpaoli & Basser, 1996); mean diffusivity (MD, omnidirectional diffusion); axial diffusivity (D_A , parallel diffusion); and radial diffusivity (D_R , perpendicular diffusion).

We also studied tensor skewness (Basser, 1997). Normalized tensor skewness (TSkew) was termed a “fiber-crossing index” in a study of Williams Syndrome (Marenco, et al., 2007). TSkew quantifies a distinct component of tensor shape not captured by FA or the other coefficients. Figure 1 shows prolate versus oblate tensor shapes generated at the same FA value close to our sample mean. Geometrically, TSkew and its hemispheric asymmetry index, which we name “SkewX”, quantify the degree of directional diffusion coherence (prolate tensor shape, or “linear anisotropy”) versus the degree of diffusion in tangent directions (oblate tensor shape, or “planar anisotropy”) (Alexander, Hasan, Kindlmann, Parker, & Tsuruda, 2000; Criscione, Humphrey, Douglas, & Hunter, 2000; Ennis & Kindlmann, 2006).

Previously, we found strong autism-control differences between tensor coefficients in the superior temporal gyrus (STG) and temporal stem (TS), two structures containing WM fibers critically involved in language and social cognition (Lee et al, 2007). In the present

study, we investigated the ability of tensor coefficients in the STG and TS to correctly discriminate individuals with autism from typically developing individuals.

METHODS AND MATERIALS

Participants

WMM measurements were further examined from thirty high-functioning (performance IQ (PIQ) ≥ 85) right-handed males meeting full criteria for autism and thirty typically developing and matched males who participated in a larger previous study (Lee, et al., 2007). Autism and control participants were selected based on closeness of individual matching on age, PIQ, handedness, and head circumference.

Diagnosis

Autism diagnosis was based on ADI-R (Lord, Rutter, & Le Couteur, 1994), ADOS-G (Lord, et al., 2000), DSM-IV and ICD-10 criteria. Exclusion criteria included patient history, Fragile-X, karyotype or clinical indications of medical causes of autism, history of severe head injury, hypoxia-ischemia, seizures and other neurologic disorders. Psychiatric comorbidity and medication status were not exclusion criteria for individuals with autism. Lifetime psychiatric comorbidity was identified in 53% (16/30) of our autism subjects. Of these, 56% (9) had depression, 31% (5) attention deficit/hyperactivity disorder, 25% (4) obsessive-compulsive disorder, 19% (3) anxiety disorder. Sixty-three percent (19/30) of subjects with autism were taking one or more psychotropic medications at the time of testing. Of these, 89% (17) used SSRIs, 26% (5) stimulants, 26% (5) valproic acid, 26% (5) neuroleptics. Controls were assessed with the ADOS-G, IQ, language, and other neuropsychological tests, and a standardized psychiatric measure (Leyfer, et al., 2006) to confirm typical development. All participants were verbal at the time of testing and spoke English as their first language.

Assessments

The Edinburgh Handedness Inventory (Oldfield, 1971) quantified handedness. Maximal occipital-frontal head circumference was measured. IQ was ascertained by the DAS or WISC-III for children and the WAIS-III for adults. The CELF-3 (Semel, Wiig, & Secord, 1995) and Vineland Scales (Sparrow et al, 1984) measured language and adaptive functioning. The Social Responsiveness Scale (SRS) (Constantino, Przybeck, Friesen, & Todd, 2000) quantified autistic traits. The Autism Comorbidity Interview (ACI) assessed lifetime history of comorbidity and ruled out any concurrent episode of major depression (Leyfer, et al., 2006).

Imaging protocol

Brain imaging, image quality control and regional segmentation (Figure 2) were performed as described by Lee et al. (2007).

Biostatistics

Our focus on potential pathology in the STG and TS employs a high degree of feature selection. It provides lower exploratory power than do whole-brain approaches. We considered a maximum of six tensor coefficients to preserve at least a 10:1 subject-to-feature ratio. Each tensor coefficient was summarized by its hemispheric mean, standard deviation (SD) and coefficient of variation (CV), defined as the SD expressed as a percentage of the mean. CV is preferred to SD when comparing mean-variance pairs that may differ and may be correlated (Lange, Giedd, Castellanos, Vaituzis, & Rapoport, 1997; Kennedy, Lange, Makris, Bates, Meyer, & Caviness, V. S., Jr., 1998; van Belle, Heagerty, Fisher, & Lumley,

2004), as in our sample. A hemispheric asymmetry index was defined as $2(L-R)/(L+R)$ (Galaburda, Corsiglia, Rosen, & Sherman, 1987), whose positive and negative values indicate leftward and rightward asymmetry. Test-wise false-positive error rate was set at 0.05 and all p-values were corrected by Bonferroni's method (factor of 4). We employed quadratic discriminant analysis (QDA) that included leave-one-out cross-validation and computation of Mahalanobis distances (Ripley, 1996; Lange 1999) to identify the combination of tensor coefficients that minimized group misclassification rate. We also employed a support vector machine (SVM) (Cortes & Vapnik, 1995; Koutsouleris, et al., 2009) with Gaussian kernel and leave-one-out cross-validation to compare parametric and non-parametric approaches. Classification ability was determined by an independent 30% replication sample (12 autism, 7 control). Classification reliability was assessed by the intraclass correlation coefficient (Fleiss & Cohen, 1973). All data analysis except the SVM was performed in R version 2.9.0.

RESULTS

Participant characteristics

The groups did not differ significantly with respect to age, IQ, handedness or head circumference; Table 2. As expected, the groups differed on language functioning. There was no evidence of greater subject motion in the autism sample and all image data analyzed herein passed our high-level quality control criteria (Lee, et al., 2007).

Tensor coefficients by group, structure and hemisphere

Table 3 contains mean, SD and CV of the tensor coefficients. In the STG, TSkew was greater on the left in controls and greater on the right in individuals with autism ($p=0.044$). When we accounted for statistical associations with decreased left STG FA, SkewX revealed a more significant reversal of the typical left lateralization of more prolate tensor shape in the STG (asymmetry indices: -0.0220 autism, 0.0303 control, $p=0.0199$). TSkew and SkewX were unaffected by cross-sectional age in both groups.

Group separation

The quadratic discriminant function identified by the first sample indicated that the combination of three tensor coefficients in the STG (SkewX, left FA and D_A bilaterally) and three in the right TS (D_A , D_R and MD) possessed 93.6% sensitivity, 89.6% specificity, 91.6% accuracy, 90% positive predictive value, 93.3% negative predictive value, and 83.3% reliability; Tables 4 and 5. The classification did not depend on cross-sectional age; univariate dependencies of tensor coefficients on age are found in Supplementary Material. White matter volume was not associated with classification ability. Since it is difficult without animation to visualize how all tensor coefficients combine in six dimensions, bivariate plots of tensor coefficients, ordered by their decreasing rates of correct classification, provide 2D distances of individual tensor coefficients to the discrimination hyperplane (Figure 4, left to right, top to bottom). QDA outperformed the SVM, which had lower accuracy (86.7%), positive predictive value (80.5%), and reliability (63.2%). Our comparison demonstrated the benefit of fitting a parametric model when applicable (Altham, 1984). Application of the QDA discrimination rule to the independent replication sample yielded equally high performance; Table 4. Decreased STG SkewX had the largest influence of all classifiers, followed by decreased left STG FA. When applied to the independent sample, a deficient algorithm without STG SkewX showed much poorer performance; Table 4.

Clinical correlation

The distances of individual sets of all six tensor coefficients to the classifier boundary were correlated with individual SRS scores, but did not reach statistical significance ($p=0.08$, uncorrected). Low leftward FA in the STG was associated with the composite Vineland score ($p=0.004$, uncorrected; $p = 0.024$, corrected) and high rightward perpendicular diffusion in the TS was correlated with the CELF-3 Receptive score ($p=0.018$, uncorrected) and with PIQ ($p=0.035$, uncorrected).

DISCUSSION

Our observations suggest a greater disruption of spatial organization of superior temporal gyrus (STG) and temporal stem (TS) white matter fibers in autism than has been reported previously. The principal new findings of this study are reversed asymmetry of diffusion tensor skewness in the STG in autism and very high ability of the physical properties of WMM measurements in the STG and TS to separate individuals with autism from typically developing individuals. Skewness characterizes the shape of the diffusion tensor, a component of the directional coherence of water diffusion in white matter not captured by FA. The a multivariate composition of six tensor coefficients illuminates differences in tensor skewness hemispheric asymmetry and other WMM diffusion tensor coefficients in the STG and TS that best distinguish individuals with autism from typically developing individuals.

We have no evidence that non-autistic factors account for the observed findings. Image quality was equally high in both groups. A few younger participants with autism were sedated for scanning but the group separation method performed equally well in younger and older individuals. Some autism participants had neuropsychiatric conditions in addition to autism and were taking psychotropic medications. Our results to date suggest that, in autism, psychotropic medication usage does not affect WMM (Alexander, et al., 2007; Lee, et al., 2007). The nearly significant correlation of the multivariate combination of six tensor coefficients with a quantitative trait index of autism together with significant univariate associations between tensor coefficients and measures of language, IQ and adaptive functioning provide evidence that our findings are due to autism-related differences in WMM.

Our observations have neurobiological implications. The results provide new evidence of key involvement of the STG and TS in the neurobiology of autism (Bigler, et al., 2003; Bigler, et al., 2007; Neeley, et al., 2007; Lee, et al., 2007; Lee, et al., 2009). Involvement of the STG and TS indicates atypicality in both superficial and deep white matter compartments. Hemispheric reversal of tensor shape in the STG (SkewX) is the most salient atypicality, followed by a loss of typical leftward asymmetry of STG FA. These reversals suggest that directional diffusion along white matter fibers in the STG is more coherent on the right and less coherent on the left in autism and a possible disruption of factors that affect hemispheric lateralization of WMM during development. Atypicality of different tensor coefficients in the STG and the TG suggests heterogeneity of WMM changes in autism. Clinical heterogeneity in autism may be due to neuropathological heterogeneity. Atypical increases of omnidirectional and perpendicular diffusion in the right TS may be due to differences in crossing fibers, dysmyelination, fiber packing, axonal diameter, intracellular viscosity, osmotic pressure and/or neurofibrils (Song, et al., 2002; Beaulieu and Allen, 2005; Alexander, et al., 2007). Some or all of these factors could be affected in autism and be ruled in or out by advanced imaging techniques and longitudinal data. Transposition of WMM architecture as measured by SkewX in the left and right STG in the context of increased multi-component diffusion in the right TS suggest complex interactions between superficial and deep WM compartment circuitry. The TS contains important

afferent and efferent fibers connecting the STG and other temporal lobe regions to the thalamus, homotopic regions in the contralateral hemisphere and other regions in ipsilateral and contralateral hemispheres. Interactions between STG and TS circuitry may be related to atypical structure-function relationships in the STG (Bigler, et al., 2007) and physiological dysfunction in subregions of the STG such as the auditory cortex (Roberts, et al., 2010).

A multivariate combination of six measures of atypical deviations of WMM in the STG and right TS discriminated between individuals with autism and typically developing individuals with 94% sensitivity, 90% specificity and 92% accuracy. Equally high performance was seen in a small independent replication sample. Our results demonstrate the ability of multivariate analysis of WMM to elide the artificial separation of biological factors by univariate approaches and provide a more comprehensive interpretation of the subtle facets of atypical brain circuitry found in autism. Future investigations that strike a scientifically effective balance between whole-brain exploratory approaches and *a priori* feature selection may result in even higher classification ability, reliability and predictive power.

The neuropathology of autism remains unclear. Heterogeneous and shared neuropathology could help identify the genetic etiology of the disorder. Further development and validation of our findings in longitudinal non-human animal studies and clinical settings may increase our understanding of biological mechanisms contributing to WMM atypicality that may give rise to autism.

We acknowledge the following limitations of the present work. Comparison groups of individuals with developmental disorders other than high-functioning autism are needed to determine the specificity of our results to the disorder. Our classifier employs a high degree of feature selection limiting exploratory power. Extensions of our findings to high-severity individuals with autism, infants, young children and females are unknown at present. Future studies of larger cross-sectional and longitudinal samples are essential. The regional tensor coefficients studied are ensemble averages of local tensors, which are themselves averages of thousands of axons mixed with non-myelinated tissue that blur finer anatomic distinctions. Higher-resolution DTI studies of human and non-human animals (Assaf, Blumenfeld-Katzir, Yovel, & Basser, 2008; Barazany, Basser, & Assaf, 2009) and more informative models of autism will yield further insight on relations between microscopic white matter neuropathology and clinical features and course of the disorder.

Supplementary Material

Refer to Web version on PubMed Central for supplementary material.

Acknowledgments

This work was funded by NIMH080826, NIMH084795, and Autism Speaks Awards 1677 and 2291 (JEL); NINDS34783 and NIMH60450 (NL); NICHD35476, CIBM-University of Wisconsin, MIR-Univ. Wisconsin (NA); NIH MRDDRC, NIMH62015, and NIDA15879 (ALA); and NIH/NIDCD F31DC010143 (M.B.D.); and Neuroscience Training Grant NIH NIDCD T32DC008553 (Univ. Utah). The content is solely the responsibility of the authors and does not necessarily represent the official views of the NIMH, NIDA, NINDS, NICHD, NIDCD or the NIH. We express our sincere gratitude to the children, adults and families who participated in this study.

LITERATURE CITED

Adluru N, Hinrichs C, Chung MK, Lee JE, Singh V, Bigler ED, et al. Classification in DTI using shapes of white matter tracts. *Conf Proc IEEE Eng Med Biol Soc.* 2009; 1:2719–2722. [PubMed: 19964040]

- Akshoomoff N, Lord C, Lincoln AJ, Courchesne RY, Carper RA, Townsend J, et al. Outcome classification of preschool children with autism spectrum disorders using MRI brain measures. *J Am Acad Child Adolesc Psychiatry*. 2004; 43(3):349–357. [PubMed: 15076269]
- Alexander AL, Hasan K, Kindlmann G, Parker DL, Tsuruda JS. A geometric analysis of diffusion tensor measurements of the human brain. *Magn Reson Med*. 2000; 44(2):283–291. [PubMed: 10918328]
- Alexander AL, Lee JE, Lazar M, Boudos R, DuBray MB, Oakes, et al. Diffusion tensor imaging of the corpus callosum in autism. *Neuroimage*. 2007; 34(1):61–73. [PubMed: 17023185]
- Altham PME. Improving the precision of estimation by fitting a model. *Journal of the Royal Statistical Society, Series B*. 1984; 46(1):118–119.
- Assaf Y, Blumenfeld-Katzir T, Yovel Y, Basser PJ. AxCaliber: a method for measuring axon diameter distribution from diffusion MRI. *Magn Reson Med*. 2008; 59(6):1347–1354. [PubMed: 18506799]
- Barazany D, Basser PJ, Assaf Y. In vivo measurement of axon diameter distribution in the corpus callosum of rat brain. *Brain*. 2009; 132(Pt 5):1210–1220. [PubMed: 19403788]
- Basser P. New histological and physiological stains derived from diffusion-tensor MR images. *Annals of the New York Academy of Sciences*. 1997; 820:123–138. [PubMed: 9237452]
- Basser PJ, Mattiello J, LeBihan D. MR diffusion tensor spectroscopy and imaging. *Biophysical Journal*. 1994; 66:259–267. [PubMed: 8130344]
- Basser PJ, Pierpaoli C. Microstructural and physiological features of tissues elucidated by quantitative-diffusion-tensor MRI. *J Magn Reson B*. 1996; 111(3):209–219. [PubMed: 8661285]
- Beaulieu C, Allen PS. Water diffusion in the giant axon of the squid: Implications for diffusion-weighted MRI of the nervous system. *Magn Reson Med*. 2005; 32(5):579–583. [PubMed: 7808259]
- Bigler ED, Tate DF, Neeley ES, Wolfson LJ, Miller MJ, et al. Temporal lobe, autism, and macrocephaly. *Am J Neuroradiol*. 2004; 24(10):2066–2076. [PubMed: 14625235]
- Bigler ED, Mortensen S, Neeley ES, Ozonoff S, Krasny L, Johnson M, et al. Superior temporal gyrus, language function, and autism. *Developmental Neuropsychology*. 2007; 31:217–238. [PubMed: 17488217]
- Casanova MF, El-Baz A, Mott M, Mannheim G, Hassan H, Fahmi R, et al. Reduced gyral window and corpus callosum size in autism: possible macroscopic correlates of a minicolumnopathy. *J Autism Dev Disord*. 2009; 39(5):751–764. [PubMed: 19148739]
- Catani M, Allin MP, Husain M, Pugliese L, Mesulam MM, Murray RM, et al. Symmetries in human brain language pathways correlate with verbal recall. *Proc Natl Acad Sci U S A*. 2007; 104(43):17163–17168. [PubMed: 17939998]
- Catani M, ffytche DH. The rises and falls of disconnection syndromes. *Brain*. 2005; 128(Pt 10):2224–2239. [PubMed: 16141282]
- Chang LC, Jones DK, Pierpaoli C. RESTORE: Robust estimation of tensors by outlier rejection. *Magn Reson Med*. 2005; 53:1088–1095. [PubMed: 15844157]
- Constantino JN, Przybeck T, Friesen D, Todd RD. Reciprocal social behavior in children with and without pervasive developmental disorders. *J Dev Behav Pediatr*. 2000; 21(1):2–11. [PubMed: 10706343]
- Cortes C, Vapnik V. Support vector networks. *Machine Learning*. 1995; 20(3):273–297.
- Criscione JC, Humphrey JD, Douglas AS, Hunter WC. An invariant basis for natural strain which yields orthogonal stress response terms in isotropic hyperelasticity. *J Mech Phys Sol*. 2000; 48:2445–2465.
- Ecker C, Rocha-Rego V, Johnston P, Mourao-Miranda J, Marquand A, Daly EM, et al. Investigating the predictive value of whole-brain structural MR scans in autism: a pattern classification approach. *Neuroimage*. 49(1):44–56. [PubMed: 19683584]
- Ennis DB, Kindlmann G. Orthogonal tensor invariants and the analysis of diffusion tensor magnetic resonance images. *Magn Reson Med*. 2006; 55(1):136–146. [PubMed: 16342267]
- Fan X, Miles JH, Takahashi N, Yao G. Abnormal transient pupillary light reflex in individuals with autism spectrum disorders. *J Autism Dev Disord*. 2009; 39(11):1499–1508. [PubMed: 19499319]

- Flagg EJ, Cardy JE, Roberts W, Roberts TP. Language lateralization development in children with autism: insights from the late field magnetoencephalogram. *Neurosci Lett*. 2005; 386(2):82–87. [PubMed: 16046066]
- Fleiss JL, Cohen J. The equivalence of weighted kappa and the intraclass correlation coefficient as measures of reliability. *Educational and Psychological Measurement*. 1973; 33:613–619.
- Galaburda AM, Corsiglia J, Rosen GD, Sherman GF. Planum temporale asymmetry, reappraisal since Geschwind and Levitsky. *Neuropsychologia*. 1987; 25(6):853–868.
- Hickok G, Poeppel D. Towards a functional neuroanatomy of speech perception. *Trends Cogn Sci*. 2000; 4(4):131–138. [PubMed: 10740277]
- Jiao Y, Chen R, Ke X, Chu K, Lu Z, Herskovits EH. Predictive models of autism spectrum disorder based on brain regional cortical thickness. *Neuroimage*. 2010; 50(2):589–599. [PubMed: 20026220]
- Kennedy DN, Lange N, Makris N, Bates J, Meyer J, Caviness VS Jr. Gyri of the human neocortex: an MRI-based analysis of volume and variance. *Cereb Cortex*. 1998; 8(4):371–384.
- Kleinhans NM, Muller RA, Cohen DN, Courchesne E. Atypical functional lateralization of language in autism spectrum disorders. *Brain Res*. 2008; 1221:115–125. [PubMed: 18555209]
- Koutsouleris N, Meisenzahl EM, Davatzikos C, Bottlender R, Frodl T, Scheuerecker J, et al. Use of neuroanatomical pattern classification to identify subjects in at-risk mental states of psychosis and predict disease transition. *Arch Gen Psychiatry*. 2009; 66(7):700–712. [PubMed: 19581561]
- Lainhart, JE.; Lange, N. The Biological Broader Autism Phenotype. In: Amaral, D.; Dawson, G.; Geschwind, D., editors. *Autism Spectrum Disorders*. Oxford: Oxford University Press; in press
- Lange N, Giedd JN, Castellanos FX, Vaituzis AC, Rapoport JL. Variability of human brain structure size: ages 4–20 years. *Psychiatry Res*. 1997; 74(1):1–12. [PubMed: 10710158]
- Lange, N. Pattern recognition. In: Armitage, P.; Colton, T., editors. *Encyclopedia of Biostatistics*. Vol. 5. 1999. p. 3298–3304.
- Lee JE, Bigler ED, Alexander AL, Lazar M, DuBray MB, Chung MK, et al. Diffusion tensor imaging of white matter in the superior temporal gyrus and temporal stem in autism. *Neurosci Lett*. 2007; 424(2):127–132. [PubMed: 17714869]
- Lee JE, Chung MK, Lazar M, DuBray MB, Kim J, Bigler ED, et al. A study of diffusion tensor imaging by tissue-specific, smoothing-compensated voxel-based analysis. *Neuroimage*. 2009; 44(3):870–873. [PubMed: 18976713]
- Leyfer OT, Folstein SE, Bacalman S, Davis NO, Dinh E, Morgan J, et al. Comorbid psychiatric disorders in children with autism: interview development and rates of disorders. *J Autism Dev Disord*. 2006; 36(7):849–861. [PubMed: 16845581]
- Lord C, Risi S, Lambrecht L, Cook EH Jr, Leventhal BL, DiLavore PC, et al. The autism diagnostic observation schedule-generic: a standard measure of social and communication deficits associated with the spectrum of autism. *J Autism Dev Disord*. 2000; 30(3):205–223. [PubMed: 11055457]
- Lord C, Rutter M, Le Couteur A. Autism Diagnostic Interview-Revised: a revised version of a diagnostic interview for caregivers of individuals with possible pervasive developmental disorders. *J Autism Dev Disord*. 1994; 24(5):659–685. [PubMed: 7814313]
- Marenco S, Siuta MA, Kippenhan JS, Grodofsky S, Chang WL, Kohn P, et al. Genetic contributions to white matter architecture revealed by diffusion tensor imaging in Williams syndrome. *Proc Natl Acad Sci U S A*. 2007; 104(38):15117–15122. [PubMed: 17827280]
- Neeley ES, Bigler ED, Krasny L, Ozonoff S, McMahon W, Lainhart JE. Quantitative temporal lobe differences: autism distinguished from controls using classification and regression tree analysis. *Brain Dev*. 2007; 29(7):389–399. [PubMed: 17204387]
- Oldfield RC. The assessment and analysis of handedness: the Edinburgh inventory. *Neuropsychologia*. 1971; 9(1):97–113. [PubMed: 5146491]
- Pierpaoli C, Basser PJ. Toward a quantitative assessment of diffusion anisotropy. *Magn Reson Med*. 1996; 6:893–906. [published erratum appears in *Magn Reson Med* 1997 Jun;37(6):972]. [PubMed: 8946355]
- Reynolds, CR.; Bigler, ED. *Test of Memory and Learning*. Austin, TX: PRO-ED; 1994.
- Ripley, BD. *Pattern Recognition and Neural Networks*. New York: Cambridge University Press; 1996.

- Roberts TP, Khan SY, Rey M, Monroe JF, Cannon K, Blaskey L, et al. MEG detection of delayed auditory evoked responses in autism spectrum disorders: towards an imaging biomarker for autism. *Autism Res.* 2010; 3(1):8–18. [PubMed: 20063319]
- Semel, E.; Wiig, EH.; Secord, WA. *Clinical Evaluation of Language Fundamentals - 3rd Edition (CELF-3)*. San Antonio, TX: Psychological Corporation; 1995.
- Singh V, Mukherjee L, Chung MK. Cortical surface thickness as a classifier: boosting for autism classification. *Med Image Comput Comput Assist Interv.* 2008; 11(Pt 1):999–1007. [PubMed: 18979843]
- Song SK, Sun SW, Ramsbottom MJ, Chang C, Russell J, Cross AH. Dysmyelination revealed through MRI as increased radial (but unchanged axial) diffusion of water. *Neuroimage.* 2002; 17(3):1429–1436. [PubMed: 12414282]
- Sparrow, SS.; Balla, DA.; Cicchetti, DV. *Vineland Adaptive Behavior Scales: Interview Edition, Survey Form Manual*. Circle Pines, MN: American Guidance Service; 1984.
- van Belle, G.; Heagerty, PJ.; Fisher, LD.; Lumley, TS. *Biostatistics: A Methodology for the Health Sciences*. New York: Wiley-Interscience; 2004.
- Wilson TW, Rojas DC, Reite ML, Teale PD, Rogers SJ. Children and adolescents with autism exhibit reduced MEG steady-state gamma responses. *Biol Psychiatry.* 2007; 62(3):192–197. [PubMed: 16950225]

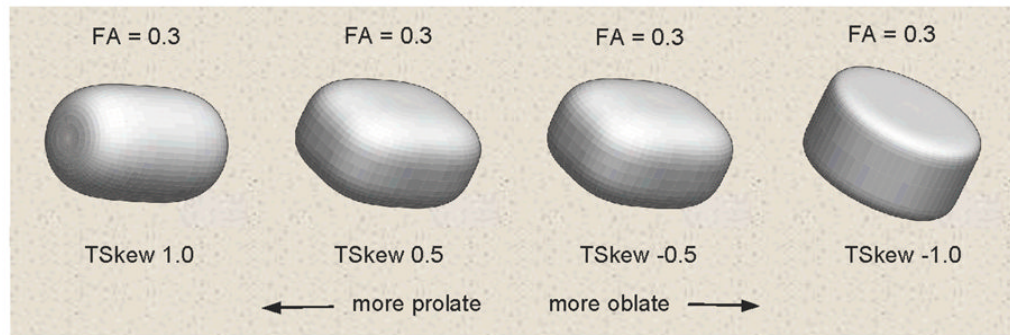


Figure 1. Example tensor skewness (TSkew) shapes over the skewness range. All shapes have the same fractional anisotropy level (FA).

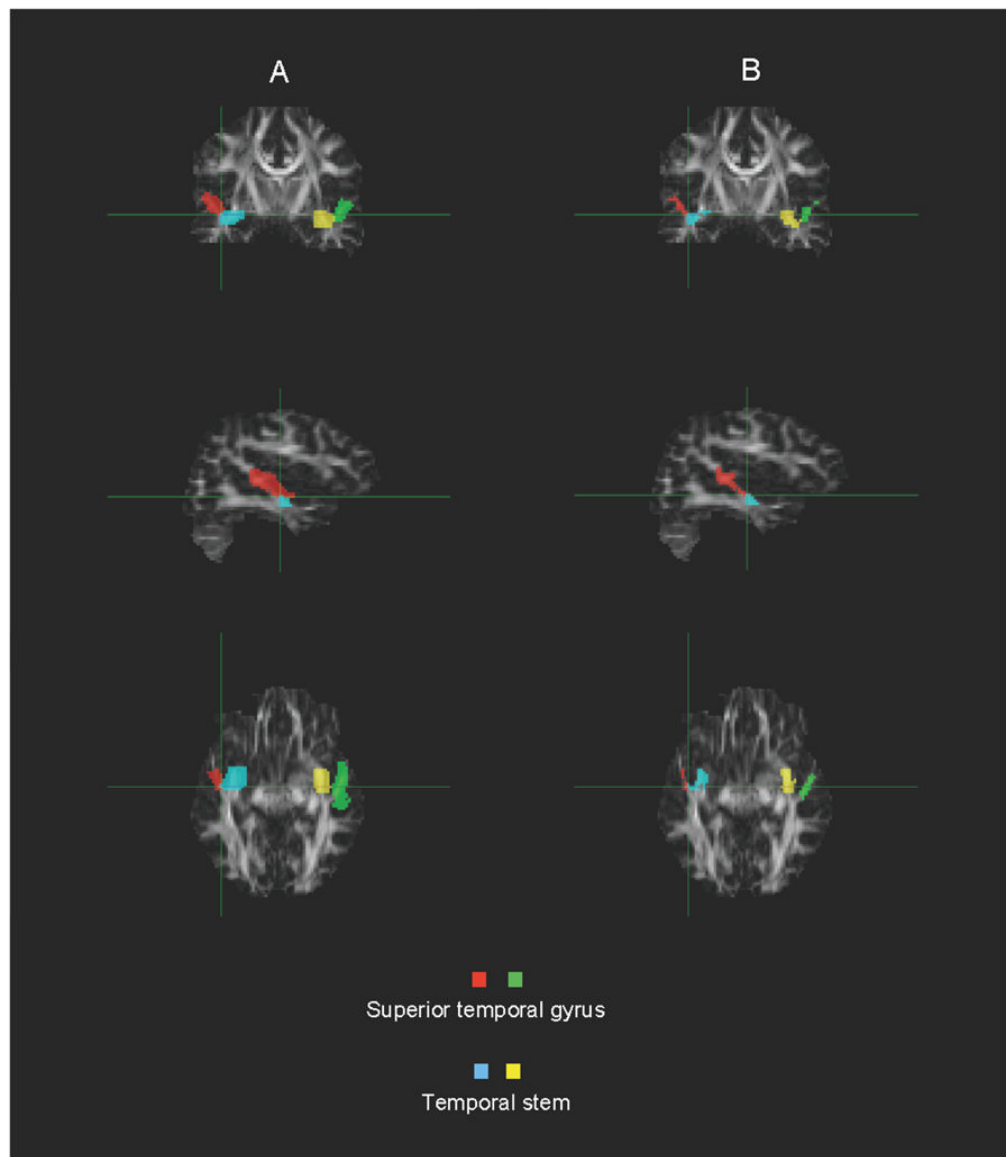


Figure 2.
Example segmentation of the superior temporal gyrus and temporal stem.
A. Raw
B. Masked for white matter only

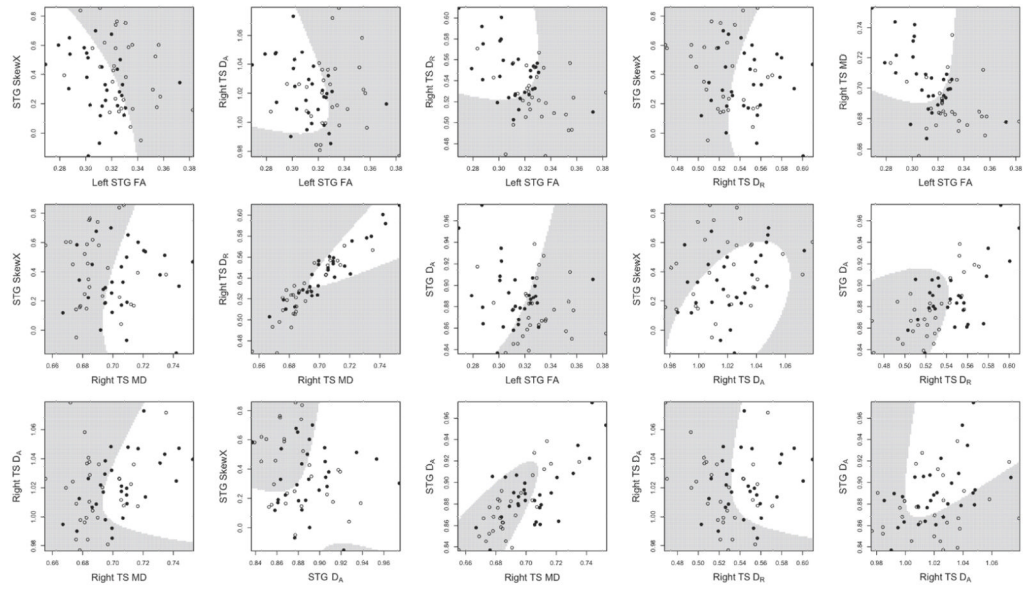


Figure 3. Bivariate plots of the six-dimensional multivariate classifier. Typically developing control values are indicated by open circles, individuals with autism by filled circles. White regions correspond to the combination of tensor coefficients that identifies an individual with autism.

Table 1

Biological classification results in autism spectrum disorders.

Biological Characteristic	Measurement Type	Brain Regions	ASD/AUT*	TD Control*	Sensitivity (%)	Specificity (%)	Reference
GM and WM	Volume and area	Cerebrum, cerebellum	30 LFA, 12 HFA	32	94.7	92.3	Akshoomoff et al. 2004
GM, WM	Volume	L fusiform gyrus, R temporal stem, and R inferior temporal gyrus	33 HFA	24	85.0	83.0	Neeley et al. 2007
GM	Cortical thickness	40,000 region-specific locations	16 HFA	11	89.0	Accuracy	Singh et al. 2008
WM	Size distribution	Gyral window	14 (HFA & LFA)	28	67.0	89.0	Casanova et al. 2009
Papillary light reflex	Infra-red pupillography	-	24 ASD	43	91.7	93.0	Fan et al. 2009
GM	Cortical thickness	33 regions by hemisphere	22 ASD	16	95.0	75.0	Jiao et al. 2009
GM	Volume	33 regions by hemisphere	22 ASD	16	77.0	69.0	Jiao et al. 2009
WM fibers	Shape	-	41 HFA	32	72.0	72.0	Adlunu et al. 2009
GM	MRI network pattern classification	Frontal, temporal, parietal, and cerebellar systems	22 ASD	22	77.0	86.0	Ecker et al. 2010
WM	MRI network pattern classification	Frontal, temporal, parietal, and cerebellar systems	22 ASD	22	73.0	64.0	Ecker et al. 2010
GM & WM	MRI network pattern classification	Frontal, temporal, parietal, and cerebellar systems	22 ASD	22	77.0	77.0	Ecker et al. 2010
Auditory cortex	MEG latency delay	Superior temporal gyrus	25 ASD**	17	75.0	81.0	Roberts et al. 2010
Speech acts	Vocalization analysis	-	AUT non-AUT delay v. TD		Accuracy	77.0 – 90.0	Xu et al. 2009

* All male, except for Jiao (2009), 22 ASD (19M, 3F) and 16 TD (13M, 3F).

** 19 without language impairment, 6 with language impairment.

Table 2

Physical and cognitive ability characteristics of the sample.

	Control (n = 30)		Autism (n = 30)		Between-group Comparison		
	Mean (SD)	Range	Mean (SD)	Range	t value	P value	
Age (years)	15.79 (5.5)	8.1–26.3	15.78 (5.6)	7.0–27.8	0.10	n.s.*	
Head Circumference [†]	56.00 (2.1)	52–59	56.63 (2.3)	53–60	1.13	n.s.	
Handedness [‡]	75.17 (24.9)	6–100	80.07 (22.6)	13–100	0.48	n.s.	
	Intelligence Quotient						
Full-scale IQ	115.13 (12.9)	94–135	109.57 (16.7)	80–140	1.40	n.s.	
Performance IQ	112.77 (12.5)	90–134	109.43 (13.5)	85–135	0.88	n.s.	
Verbal IQ	112.80 (13.2)	90–140	106.63 (21.6)	70–145	1.34	n.s.	
	Language Functioning [§]						
Total	109.5 (13.2)	84–137	91.34 (21.3)	50–123	3.85	<0.001	
Receptive	110.0 (15.9)	82–143	93.85 (24.7)	50–125	2.76	0.008	
Expressive	106.9 (12.2)	82–131	90.22 (20.0)	50–120	3.58	0.001	
SRS ^{**}	15.9 (13.1)	0–48	99.61 (24.0)	34–148	15.93	<0.001	

* Not statistically significant at false-positive error rate 0.05 and p-value greater than 0.20

[†] Control: n = 27, Autism: n = 28

[‡] Edinburgh Handedness Inventory, range –100 (left handed) to 100 (right handed)

[§] Clinical Evaluation of Language Fundamentals (CELF-3); control: n = 28, Autism: n = 30

^{**} Social Responsiveness Scale (child) or Social Reciprocity Scale (adult), range 0 (no autistic-like traits) to 195 (many severe autistic traits). Control n = 27, autism n = 28. Verification of the 7 subjects having SRS scores less than 85 (SRS score 34, 1; 62–72, 2; 76–84, 4) confirmed that they met full diagnostic criteria for autism.

Table 3

Tensor coefficients and asymmetry indices by group and hemisphere. SD: standard deviation; CV: coefficient of variation; FA: fractional anisotropy; MD: mean diffusivity; D_A: axial diffusivity; D_R: radial diffusivity.

f	Typically developing (TD) N = 30				Autism N = 30				Autism - TD			
	Left Mean (SD) CV†	Right Mean (SD) CV	AI* Mean (SD) CV	Left Mean (SD) CV	Right Mean (SD) CV	AI Mean (SD) CV	Left Mean (SD) CV	Right Mean (SD) CV	Left Mean (SD)	Right Mean (SD)	AI Mean (SD)	
Superior temporal gyrus												
Skewness	0.517 (0.049) 0.095	0.502 (0.052) 0.103	0.0303 (0.0969) 3.1956	0.505 (0.040) 0.078	0.517 (0.049) 0.095	-0.0220 (0.1009) 4.5838	-0.012 (0.063)	0.015 (0.071)	-0.012 (0.063)	0.015 (0.071)	-0.0523 (0.1399)	
FA	0.339 (0.020) 0.059	0.327 (0.024) 0.073	0.0373 (0.0529) 1.4182	0.318 (0.024) 0.075	0.318 (0.018) 0.057	-0.0024 (0.0582) ∅‡	-0.021 (0.031)	-0.009 (0.030)	-0.021 (0.031)	-0.009 (0.030)	-0.0397 (0.0786)	
MD (mm²/s)	0.657 (0.027) 0.041	0.644 (0.020) 0.031	0.0194 (0.0253) 1.3041	0.671 (0.027) 0.040	0.661 (0.029) 0.044	0.0142 (0.0162) 1.1408	0.014 (0.038)	0.017 (0.035)	0.014 (0.038)	0.017 (0.035)	-0.0052 (0.0300)	
D_A (mm²/s)	0.900 (0.035) 0.039	0.870 (0.025) 0.029	0.0336 (0.0380) 1.1310	0.900 (0.031) 0.034	0.888 (0.035) 0.039	0.0132 (0.0337) 2.5530	0.000 (0.047)	0.018 (0.043)	0.000 (0.047)	0.018 (0.043)	-0.0204 (0.0508)	
D_R (mm²/s)	0.535 (0.027) 0.050	0.531 (0.023) 0.043	0.0074 (0.0232) 3.1351	0.556 (0.030) 0.054	0.548 (0.029) 0.053	0.01500 (0.0192) 1.2800	0.021 (0.040)	0.017 (0.037)	0.021 (0.040)	0.017 (0.037)	0.0076 (0.0301)	
Temporal stem												
Skewness	0.622 (0.032) 0.051	0.627 (0.035) 0.057	0.0080 (0.0644) 8.0024	0.620 (0.035) 0.057	0.611 (0.032) 0.052	0.0142 (0.0628) 4.4075	-0.002 (0.047)	-0.016 (0.047)	-0.002 (0.047)	-0.016 (0.047)	0.0062 (0.0900)	
FA	0.401 (0.021) 0.052	0.383 (0.019) 0.050	0.0463 (0.0384) 0.8294	0.386 (0.019) 0.049	0.370 (0.022) 0.059	0.0439 (0.0440) 1.0023	-0.015 (0.028)	-0.013 (0.029)	-0.015 (0.028)	-0.013 (0.029)	-0.0024 (0.0584)	
MD (mm²/s)	0.701 (0.020) 0.029	0.702 (0.019) 0.027	-0.0028 (0.0177) ∅	0.714 (0.020) 0.028	0.717 (0.023) 0.032	-0.0037 (0.0162) ∅	0.013 (0.028)	0.015 (0.030)	0.013 (0.028)	0.015 (0.030)	-0.0009 (0.0240)	
D_A (mm²/s)	1.018 (0.028) 0.028	1.001 (0.020) 0.020	0.0164 (0.0225) 1.3720	1.023 (0.021) 0.021	1.010 (0.022) 0.022	0.0128 (0.0143) 1.1172	0.005 (0.035)	0.009 (0.030)	0.005 (0.035)	0.009 (0.030)	-0.0036 (0.0267)	
D_R (mm²/s)	0.542 (0.022) 0.041	0.553 (0.023) 0.042	-0.0205 (0.0252) 1.2293	0.560 (0.023) 0.041	0.570 (0.027) 0.047	-0.0184 (0.0272) 1.4783	0.018 (0.032)	0.017 (0.035)	0.018 (0.032)	0.017 (0.035)	0.0021 (0.0371)	

Table 4

Group separation ability of the multivariate collection of diffusion tensor coefficients with and without tensor skewness hemispheric asymmetry (SkewX).

	First Sample		Second Sample	
	30 Autism	30 Control	12 Autism	7 Control
	With SkewX*	Without SkewX	With SkewX	Without SkewX
Sensitivity (%)	93.6	85.9	91.7	66.7
Specificity (%)	89.6	85.2	100	71.4
Accuracy (%)	91.6	85.6	94.7	68.4
PPV [†] (%)	90.0	65.6	100	80.0
NPV [‡] (%)	93.3	71.5	87.5	55.6
Reliability ^{**} (%)	83.3	68.9	89.0	36.0

* Inter-hemispheric asymmetry of tensor skewness

[†] Positive predictive value

[‡] Negative predictive value

** Intraclass correlation coefficient

Table 5

A potential DTI “signature” for autism.

	STG	TS
Low	SkewX Left FA	-
High	D _A	Right MD Right D _A Right D _R